International Journal of Bifurcation and Chaos, Vol. 26, No. 7 (2016) 1650121 (11 pages)

DOI: 10.1142/S0218127416501212

Chaotic Map Construction from Common Nonlinearities and Microcontroller Implementations

Günyaz Ablay
Department of Electrical-Electronics Engineering,
Abdullah Gül University, Kayseri 38080, Turkey
gunyaz.ablay@agu.edu.tr

Received December 20, 2015; Revised February 14, 2016

This work presents novel discrete-time chaotic systems with some known physical system nonlinearities. Dynamic behaviors of the models are examined with numerical methods and Arduino microcontroller-based experimental studies. Many new chaotic maps are generated in the form of $x(k+1) = rx(k) + f(x(k))$ and high-dimensional chaotic systems are obtained by weak coupling or cross-coupling the same or different chaotic maps. An application of the chaotic maps is realized with Arduino for chaotic pulse width modulation to drive electrical machines. It is expected that the new chaotic maps and their microcontroller implementations will facilitate practical chaos-based applications in different fields.

Keywords: Chaos; discrete chaos; chaotic map; random number; microcontroller.

1. Introduction

Chaotic maps or discrete-time chaotic systems arise in different ways, including as models of natural events, as examples of chaos and as tools in the analysis of dynamical systems. Maps have allowed some successful estimate on the routes to chaos in heart cells, chemical oscillators, lasers, fluid dynamics and semiconductors [Tsonis, 1996; Strogatz, 2014; Ruelle, 1997]. Discrete-time chaotic systems have found a wide-range of applications in many disciplines, for instance, cryptography, engineering, physics, biology and philosophy. Some successful applications include digital watermarking, random number generation (e.g. used in Monte Carlo methods), chaos-based scheduling in wireless sensor networks, etc. [Bahi & Guyeux, 2013].

The useful chaos implementations have created increasing interest in various chaos-based applications and a huge demand for novel chaos generators with simple designs. Some examples of chaotic maps include logistic map, cubic map, Ricker's map, sine map, Henon map, Gingerbreadman map, Burgers' map, tinkerbell map, shift map, tent map, Arnolds cat map and Bakers map [Strogatz, 2014; Bahi & Guyeux, 2013; Atay *et al.*, 2009; Sprott, 2001; Chen & Huang, 2011]. In recent years, new discrete-time chaotic systems have also been proposed, for example, chaos in periodic discrete systems [Shi *et al.*, 2015], nonautonomous discrete systems [Shi, 2012], Chua machines [Bilotta & Pantano, 2009], neural networks [Chen *et al.*, 2007], some modified logistic maps [Acho, 2015; Radwan, 2013; Liu & Miao, 2015], delayed q-deformations based chaotic maps [Shrimali & Banerjee, 2013], composition of permutations based maps [Lambi, 2015] and fractional-order chaotic maps [Wu & Baleanu, 2013; Wu *et al.*, 2014]. In addition, high-dimensional chaotic maps have been generated by weakly coupling some low-dimensional ones [Wang & Bao, 2013; Pal *et al.*, 2014; Hussain & Gondal, 2014; Tian & Chen, 2007; Willeboordse, 2003].

In this work, new discrete-time chaotic systems based on common physical nonlinearities are introduced. The weakly coupling and cross-coupling of different chaotic maps have also been studied for generating high-dimensional chaotic systems.

The novel chaotic maps are implemented via the Arduino microcontroller for generating chaotic pulse width modulation (or random numbers) for electric drive systems. Arduino is an open-source hardware on a single board and has been used in many different applications [Faugel & Bobkov, 2013; Hamiche *et al.*, 2015; Ortega-Zamorano *et al.*, 2014; Fatehnia *et al.*, 2016; Ferdoush & Li, 2014]. With this reasonably priced and easy to use tool, the existence of the chaotic maps developed in this work is shown with practical applications. The following sections present the novel chaotic maps, their coupling and implementations, and a conclusion to the paper.

2. Chaotic Maps from Common Nonlinearities

A discrete-time chaotic system with a constant parameter may be described by

$$x(k+1) = rx(k) + f(x(k)) \tag{1}$$

where r is a real-valued parameter and f is a real smooth function, $f : R \to R$. The existence of chaos in the system (1) can be shown with the positive Lyapunov exponents, bifurcation diagrams and web diagrams. Bifurcation and web diagrams will be provided in the following subsections to describe the chaotic systems. As the measurement of sensitive dependence on initial conditions, a positive Lyapunov exponent is a sign of chaos. For (1), the Lyapunov exponent (LE) can be calculated from

$$\lambda = \frac{1}{n} \lim_{n\to\infty} \sum_{i=0}^{n-1} \ln |r + f'(x_i)|. \tag{2}$$

System (1) with various simple physical nonlinear terms will serve as reference structures in the following sections for developing novel chaotic maps.

2.1. *Chaotic maps with exponential nonlinearities*

Exponential nonlinearities are commonly used in the description of diode or diode-like electronic components. The physical forms of the exponential terms can also be found in chaotic circuits and be used to get chaotic maps. Consider a discrete map in the form of (1) described by

$$x(k+1) = -rx(k) + [e^{x(k)} - 1] \tag{3}$$

where $r > 0$. The discrete system (3) has two fixed points at $x_e = (0, \gamma)$ in which the origin is stable (γ is the solution of $e^{\gamma} - r\gamma - \gamma - 1 = 0$, and $\gamma > 0$ when $r > 0$). For an initial condition $x_0 > \gamma$, the existence of chaos can be shown with the positive LEs, bifurcation diagrams and web diagrams. A bifurcation diagram exhibiting a period-doubling route to chaos for the new chaotic map (3) is shown in Fig. 1(a) for r versus $x(k)$. The existence of positive LE is also shown in the same figure. There is an interleaving of chaos and order for $2.45 < r < 2.7$. The web diagram and time-series of the chaotic map for $r = 2.6$ are illustrated in Fig. 2. All numerical results are obtained by using MATLAB/Simulink programs.

Similar to (3), some other chaotic maps with simple exponential nonlinearities can be found in the following forms:

$$x(k+1) = -rx(k) + x(k)e^{-x(k)} \tag{4}$$

$$x(k+1) = -rx(k) + e^{x(k)}. \tag{5}$$

Bifurcation diagram and LE of (4) are displayed in Fig. 1(b). Similarly, for the map (5), a chaotic

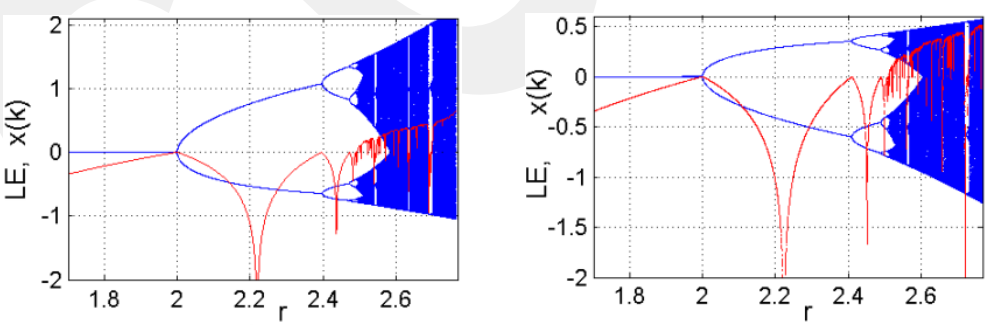

(a) (b)

Fig. 1. Lyapunov exponents and bifurcation diagrams of the chaotic maps, (a) for the map $x(k+1) = -rx(k) + \exp(x(k)) - 1$ and (b) for the map $x(k+1) = -rx(k) + x(k) * \exp(-x(k))$.

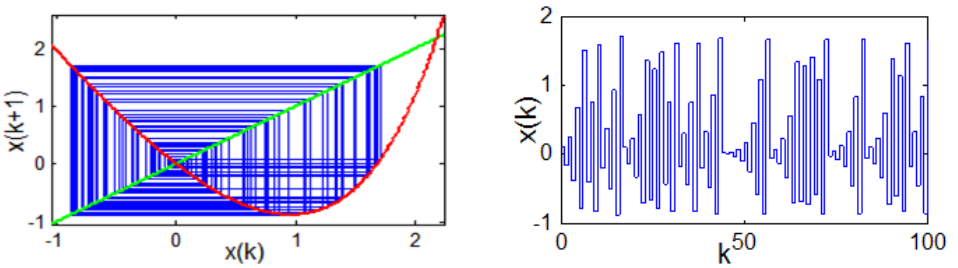

(a) (b)

Fig. 2. Web diagram and time-response of the chaotic map $x(k+1) = -rx(k) + \exp(x(k)) - 1$ for $r = 2.6$.

region exists for $2.9 < r < 3.2$. All these chaotic maps exhibit some similarities in their behaviors, but their parameter ranges and magnitude variations are completely different.

2.2. *Chaotic maps with hyperbolic–trigonometric nonlinearities*

In this subsection, chaotic maps obtained from simple hyperbolic and trigonometric functions are going to be introduced, while sinusoidal nonlinearity based simple chaotic maps exist in literature [Sprott, 2000; Ikeda & Matsumoto, 1987]. Let a discrete system be defined by

$$x(k+1) = rx(k) - \sinh x(k). \tag{6}$$

The discrete system (6) has three fixed points at $x_e = (0, \pm\gamma)$, where $(r-1)\gamma - \sinh\gamma = 0$ for $r > 1$, with stable nonzero fixed points. The bifurcation diagram of (6) exhibits a period-doubling route to chaos seen in Fig. 3(a). The positive LE also provides evidence on the existence of chaos. The chaotic behavior is initially nonsymmetric, but having a symmetric feature when $r > 3.28$. The web diagram and time-series of the chaotic map for $r = 3.2$ are shown in Fig. 4.

Similarly, some other hyperbolic functions can also be used to generate chaotic maps. Some examples include,

$$x(k+1) = -rx(k) + \cosh x(k) \tag{7}$$

$$x(k+1) = -rx(k) + \tanh ax(k). \tag{8}$$

Bifurcation diagram and LE of (7) are illustrated in Fig. 3(b). Chaotic map (8) has a wide-range of different chaotic behaviors when the parameter a varies in the range of $10 \leq a \leq 100$. We will see in the following subsection (Sec. 2.3) that the signum function can be approximated to the $\tanh(\cdot)$ function when $a \gg 1$. Besides the Taylor expansion of hyperbolic functions results in polynomial functions, and thus, various chaotic maps can be obtained from these polynomials.

While there exists a simple sinusoidal nonlinearity based chaotic map in literature [Sprott, 2000; Ikeda & Matsumoto, 1987], combinations of different trigonometric terms can also exhibit some unique chaotic systems:

$$x(k+1) = rx(k) + 2.5\sin x(k) + \cos x(k) \tag{9}$$

$$x(k+1) = r\sin x(k) + \cos x(k). \tag{10}$$

The bifurcation diagrams and LEs of (9) and (10) are given in Fig. 5, which show a period-doubling

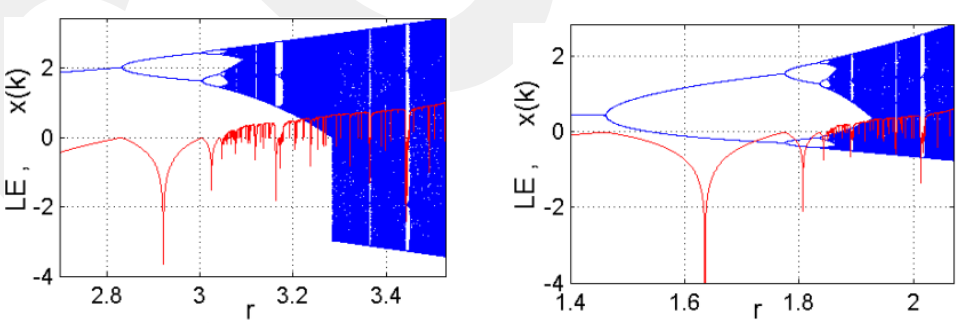

(a) (b)

Fig. 3. Lyapunov exponents and bifurcation diagrams of the chaotic maps, (a) for the map $x(k+1) = rx(k) - \sinh(x(k))$ and (b) for the map $x(k+1) = -rx(k) + \cosh(x(k))$.

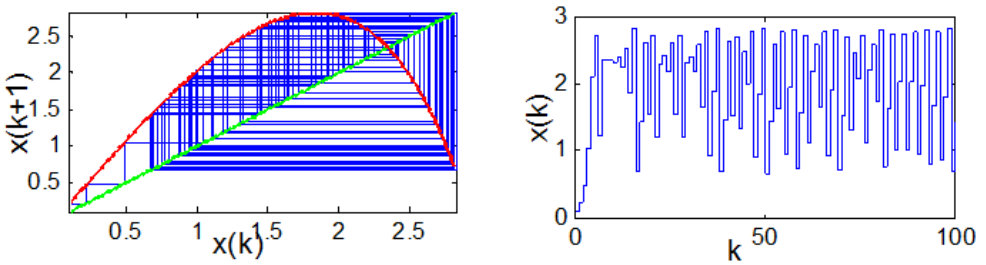

(a) (b)

Fig. 4. Web diagram and time-response of the chaotic map $x(k+1) = rx(k) - \sinh(x(k))$ for $r = 3.2$.

route to chaos. In the chaotic regions, both maps have at least three fixed points with unstable origin but stable fixed points around the origin.

2.3. *Chaotic maps with signum nonlinearities*

A chaotic map with signum nonlinearity can be defined by

$$x(k+1) = -rx(k) + \operatorname{sgn} x(k) \tag{11}$$

where the sgn(·) is the signum function defined by $\operatorname{sgn}(x) = x/|x|$ if $x \neq 0$ and $\operatorname{sgn}(x) = 0$ if $x = 0$. The sgn(·) function can also be approximated to $\operatorname{sgn}(x) \approx \tanh ax$ for $a \gg 1$ (e.g. $a = 100$) for smooth results. It is interesting to note that the signum function produces chaos in continuous-time autonomous and delay systems [Ablay, 2015b; Lakshmanan & Senthilkumar, 2010; Ablay, 2015a], and discrete systems [Acho, 2015]. The discrete system (11) has three fixed points, $x_e = (0, \pm 1/(r+1))$ for $r > 0$, where the nonzero fixed points are stable. Bifurcation diagram and LE of the map (11) are shown in Fig. 6(a) for r versus $x(k)$. There is an almost continuous chaos and order for $r > 1$. The web diagram and the time response of the chaotic map are seen in Fig. 7.

The smooth forms of the sgn(·) function can also be used to generate chaos in discrete systems, as given in the following equations:

$$x(k+1) = -rx(k) + \frac{x(k)}{|x(k)| + 0.01} \tag{12}$$

$$x(k+1) = -rx(k) + \tanh ax(k). \tag{13}$$

In (13), the parameter a in the tanh(·) function must be selected as $a \geq 100$ for getting similar results with the signum function. On the other hand, if we choose a around $10 \leq a \leq 100$, e.g. $a = 10$, completely different chaotic results are obtained as seen in Fig. 6(b).

2.4. *Chaotic maps with quadratic terms*

The quadratic nonlinearity based chaotic systems are usually known as logistic maps [Sprott, 2001]. Here are some chaotic maps with quadratic terms:

$$x(k+1) = -rx(k) + \frac{x(k)}{x(k)+1} \tag{14}$$

$$x(k+1) = rx(k) - x^2(k) \tag{15}$$

$$x(k+1) = -rx(k)[1 + x(k)]. \tag{16}$$

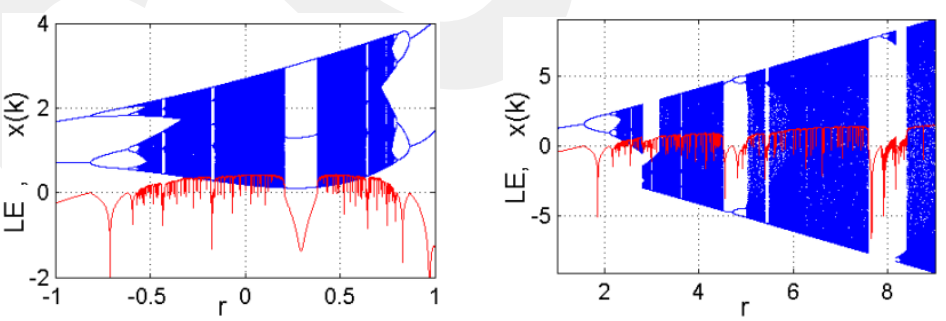

(a) (b)

Fig. 5. Lyapunov exponents and bifurcation diagrams of the chaotic maps, (a) for the map $x(k+1) = rx(k) + 2.5\sin(x(k)) + \cos(x(k))$ and (b) for the map $x(k+1) = r\sin(x(k)) + \cos(x(k))$.

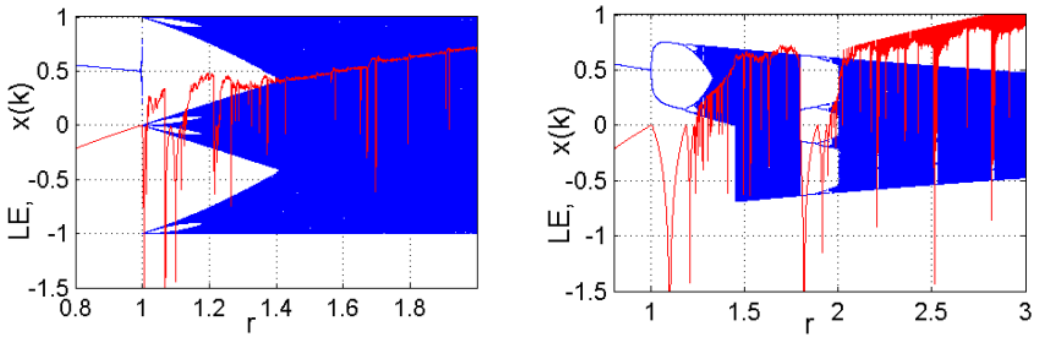

(a) (b)

Fig. 6. Lyapunov exponents and bifurcation diagrams of the chaotic maps, (a) for the map $x(k+1) = -rx(k) + \text{sgn}(x(k))$ and (b) for the map $x(k+1) = -rx(k) + \tanh(10x(k))$.

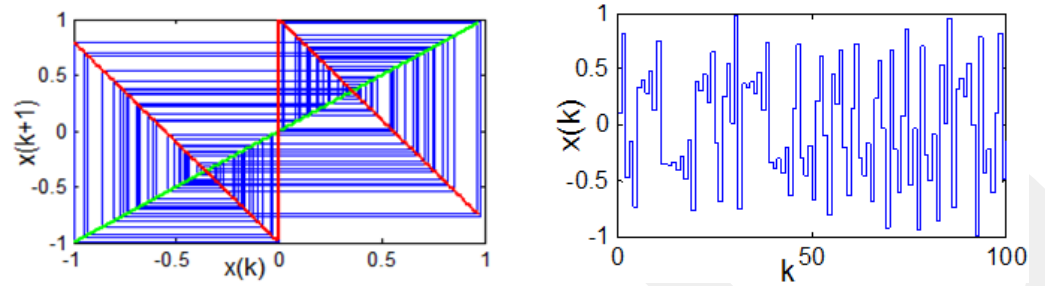

(a) (b)

Fig. 7. Web diagram and time-response of the chaotic map $x(k+1) = -rx + \text{sgn}(x)$ for $r = 1.6$.

These maps have similar chaotic features as with logistic maps. They have two fixed points with stable origin. For (14), the bifurcation diagram and LE are illustrated in Fig. 8(a), in which the results are comparable to the logistic equation. For (15), a chaotic map is found in the range of $3.5 < r < 4$, and chaos exists in (16) for $1.5 < r < 2$. It should be noted that some of the quadratic terms can be generated from the Taylor expansion of $\cosh(\cdot)$ function, e.g. $\cosh x = 1 + x^2/2$. Hence, the chaotic map (7) and the chaotic maps based on quadratic terms yield similar chaotic behaviors.

Another form of the quadratic nonlinearity can be obtained with the use of absolute value function, which can be found in nonautonomous chaotic systems [Tang *et al.*, 2001] and chaotic delay systems

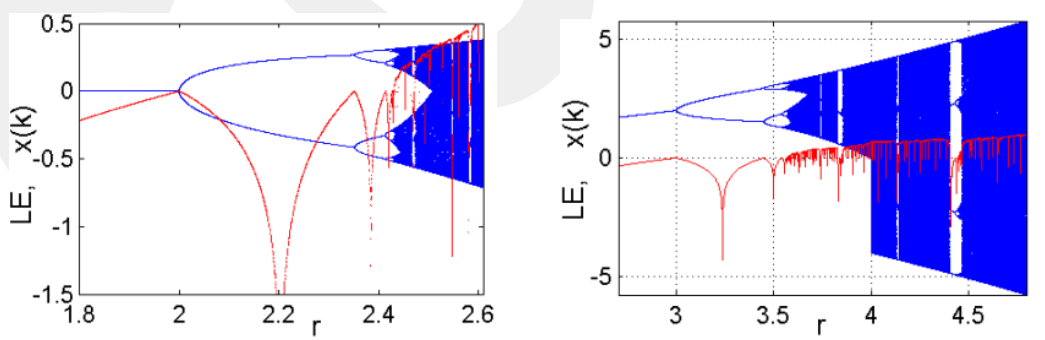

(a) (b)

Fig. 8. Lyapunov exponents and bifurcation diagrams of the chaotic maps, (a) for the map $x(k+1) = -rx(k) + x(k)/(x(k)+1)$ and (b) for the map $x(k+1) = rx(k) - x(k)|x(k)|$.

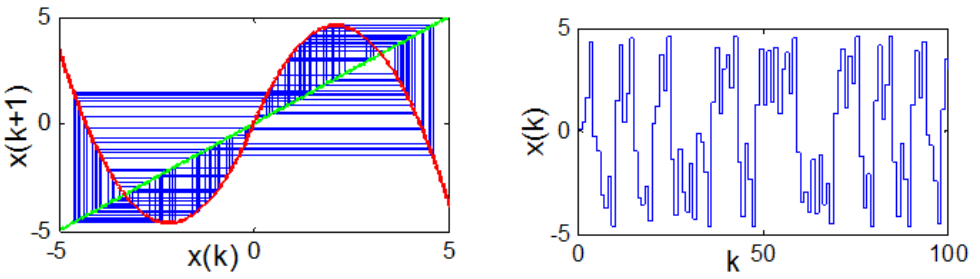

(a) (b)

Fig. 9. Web diagram and time-response of the chaotic map $x(k+1) = rx(k) - x(k)|x(k)|$ for $r = 4.1$.

[Ablay, 2015b]. Consider the following map,

$$x(k+1) = rx(k) - x(k)|x(k)|. \tag{17}$$

The bifurcation diagram and LE of (17) are shown in Fig. 8(b) where a symmetric chaotic region follows an asymmetric chaotic region. The web diagram and time response of the system are given in Fig. 9. It is clear that the absolute value nonlinearity assures rich chaotic features.

2.5. *Chaotic maps with cubic/quintic nonlinearities*

Consider a discrete map in the form of (1) described by a cubic nonlinearity

$$x(k+1) = rx(k) - x^3(k). \tag{18}$$

There are three fixed points, $x_e = (0, \pm\sqrt{r-1})$ for $r > 1$, where the nonzero fixed points are stable. Bifurcation diagram and LE of the map (18) are shown in Fig. 10(a) for r versus $x(k)$. There is an interleaving of chaos and order for $r > 2.25$. The results are similar to the chaotic map given in (6). The main reason is that the first two terms of the Taylor expansion of $\sinh(\cdot)$ function result in qubic term, $\sinh x \approx x + x^3/6$. Technically, a wide chaotic region is obtained for cubic terms for $r > 2.25$ without worrying about initial conditions.

Some other qubic/quintic chaotic maps are

$$x(k+1) = rx(k) - |x(k)|x^3(k) \tag{19}$$

$$x(k+1) = rx(k) - x^5(k). \tag{20}$$

These maps give similar results as seen in Fig. 10(b), but their parameter dependent chaotic regions are different, e.g. chaotic region of (19) can be found in the range of $1.9 < r < 2.4$.

2.6. *Chaotic maps with piecewise functions*

Consider a piecewise chaotic system described by

$$x(k+1) = rx(k) + f(x(k)) \tag{21}$$

where f is a piecewise-linear function defined by

$$f(x(k)) = \begin{cases} -4x(k) - 6, & x(k) < -1 \\ 2x(k), & -1 \le x(k) \le 1 \\ -4x(k) + 6, & x(k) > 1. \end{cases} \tag{22}$$

The function (22) is an odd piecewise-linear function. The discrete map (21) with (22) has three fixed points, $x_e = (0, \pm\gamma)$ for $r > 1$, with stable nonzero

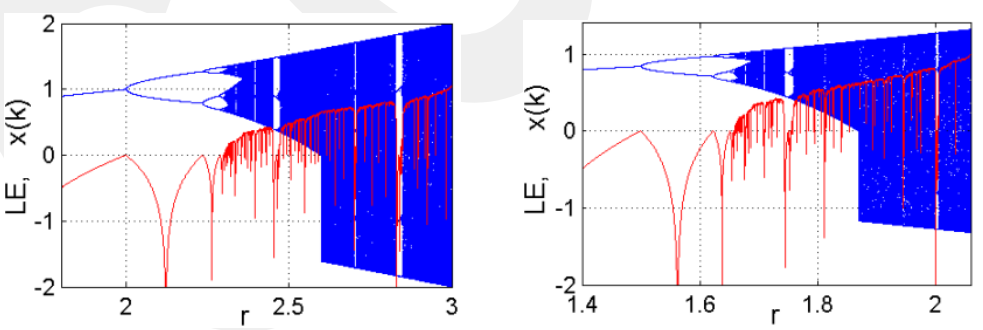

(a) (b)

Fig. 10. Lyapunov exponents and bifurcation diagrams of the chaotic maps, (a) for the map $x(k+1) = rx(k) - x^3(k)$ and (b) for the map $x(k+1) = rx(k) - x^5(k)$.

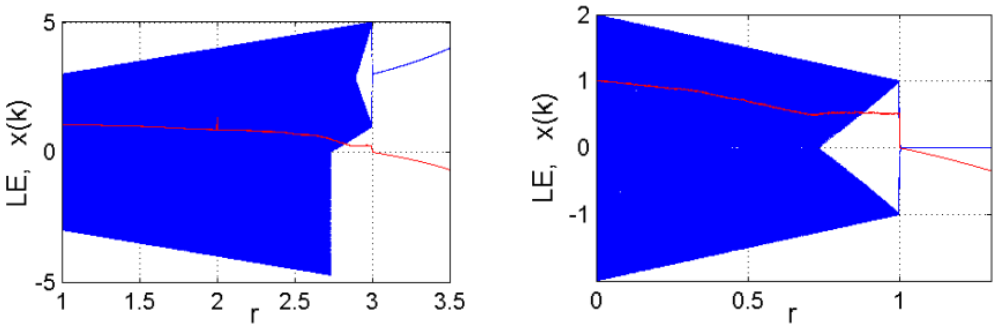

(a) (b)

Fig. 11. Lyapunov exponents and bifurcation diagrams of the chaotic maps, (a) for the map $x(k+1) = rx(k) + f(x(k))$ and (b) for the map $x(k+1) = rx(k) - f(x(k))$.

fixed points for $3 < r < 5$. The other forms of the map (21) can be written as

$$x(k+1) = \pm rx(k) \pm f(x(k)). \tag{23}$$

Bifurcation diagrams and LEs of the chaotic maps (21) and (23) are shown in Fig. 11. The chaotic region of the piecewise function based chaotic map does have a very high quality chaos without any periodic windows. Similarly, chaos exists for $x(k+1) = -rx(k) - f(x(k))$ when $1 < r < 3$, and for $x(k+1) = -rx(k) + f(x(k))$ when $0 < r < 1$.

3. Coupled Chaotic Maps

Any low-dimensional chaotic map can be extended to a high-dimensional one by weak coupling or cross-coupling some of the maps, but with varying characteristics. The usual way in such a coupling is that a chaotic map is weakly coupled with itself [Wang & Bao, 2013; Romero *et al.*, 2014]. The chaotic maps introduced in Sec. 2 can always be weakly coupled to get high-dimensional maps. On the other hand, it is also possible to couple different chaotic maps weakly. As an example, consider a diffusively coupled quadratic function (16) and signum nonlinearity (11) based chaotic maps:

$$\begin{aligned} x(k+1) &= -rx(k)[1 + x(k)] + \mu y(k) \\ y(k+1) &= -ry(k) + \operatorname{sgn} y(k) - \mu x(k) \end{aligned} \tag{24}$$

where μ is a small coupling parameter, e.g. $\mu = 0.1$. The Lyapunov exponents of the coupled map (24) are given in Fig. 12. For $1.5 < r < 2$, both $x(k)$ and $y(k)$ have chaotic behaviors. The weak coupling improves the chaotic behavior since the LEs become more positive without any periodic windows as seen in Fig. 12. Figure 13 illustrates the phase diagrams of the weakly coupled maps for $r = 1.6$, which show that dimension and randomness are improved.

The dimensions of the chaotic systems can also be increased via cross-coupling, e.g. cross-coupling of the signum nonlinearity (11) based chaotic maps can be written as,

$$\begin{aligned} x(k+1) &= -ry(k) + \operatorname{sgn} y(k) \\ y(k+1) &= -rx(k) + \operatorname{sgn} x(k) \end{aligned} \tag{25}$$

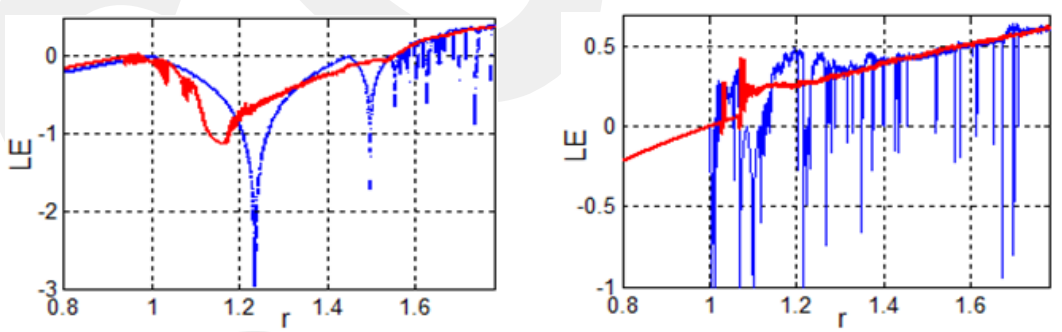

(a) (b)

Fig. 12. Comparison of the Lyapunov exponents of the one-dimensional (blue dots) and weakly coupled (red dots) chaotic maps, (a) the quadratic map and (b) the signum based chaotic map.

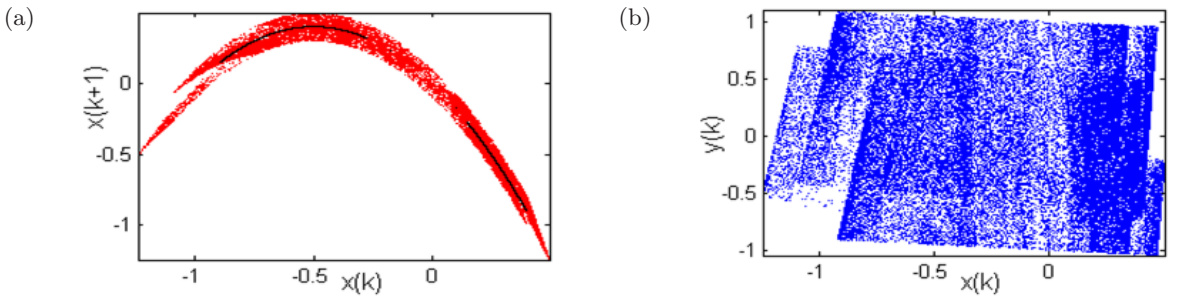

Fig. 13. Phase diagrams of the coupled chaotic maps: (a) black dots represent the quadratic map and red dots are for the coupled map and (b) $x(k)$ versus $y(k)$ plot.

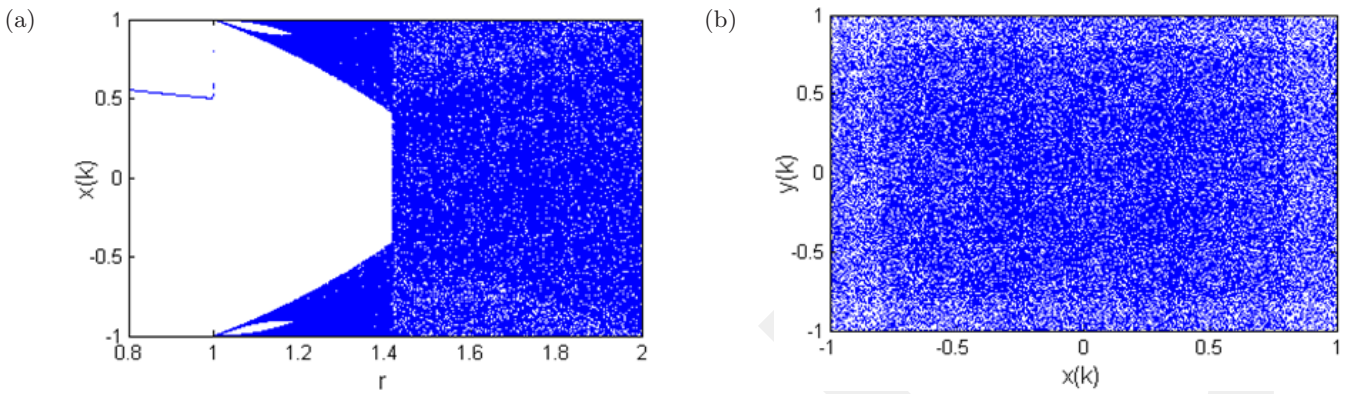

Fig. 14. Diagrams for the cross-coupled chaotic map: (a) bifurcation diagram and (b) $x(k)$ versus $y(k)$ plot.

where the initial conditions must satisfy $x_0 \neq y_0$. The bifurcation diagram and phase plot (for $r = 1.6$) of the cross-coupled chaotic system are seen in Fig. 14. It is clear that the cross-coupling enhances the randomness of the chaotic maps and allows us to generate high-dimensional chaotic maps. On the other hand, the coupling based generations of high-dimensional chaotic maps are usually *ad-hoc*.

4. Microcontroller Implementations

The novel chaotic maps can be used in many applications such as random number generators and cryptographic systems. On the other hand, an interesting application can be the chaotic pulse width modulator (PWM) for driving electrical systems. The chaotic PWM can be used for open-loop control of ac or dc motor drives, including an induction motor drive system. The main advantage of the chaotic PWM over traditional modulators is that it can reduce the effects of the electromagnetic interference problem and acoustic noise [Balestra *et al.*, 2004; Zhang *et al.*, 2012]. The chaotic PWM can also reduce the size of power filters due to its harmonic reduction feature. In the literature, chaotic PWMs are implemented by a few-tens of transistors [Delgado-Restituto & Rodriguez-Vazquez, 2002]. In this work, a simple Arduino based implementation will be introduced. Figure 15 illustrates the chaos based PWM generator (chaotic position–modulated position, modulation–sinusoidal pulse width modulation) where the control signal r is compared with a sawtooth (or triangular) signal whose frequency is f_s, and then the AND operator is applied between the chaotic sequence x and the comparator output q. The output of the AND operator can be considered as a random bit stream. Note that if we apply the chaotic sequence to the comparator input, then the PWM output, q, will have random bit series.

The Atmel ATmega328p microcontroller is the essential component of the Arduino. This microcontroller is running at 16 Mhz with an 8-bit core, and has a limited amount of available memory, with

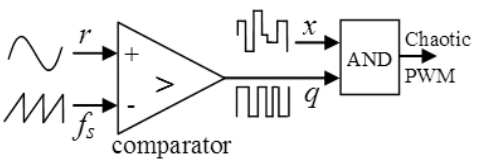

Fig. 15. Chaos based PWM.

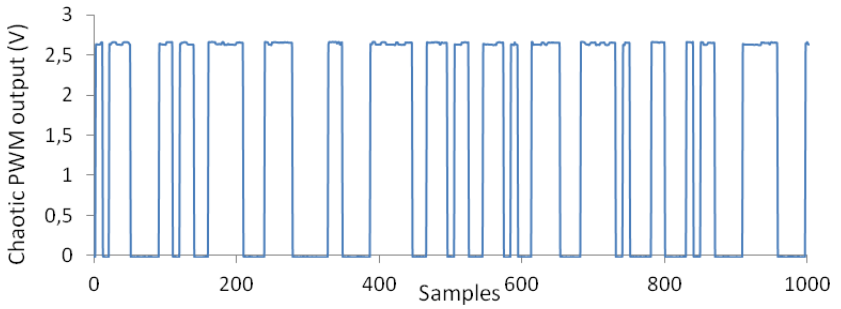

Fig. 16. Arduino results for the chaotic PWM implementation on the chaotic map $x(k+1) = -1.8x(k) + \text{sgn}(x(k))$.

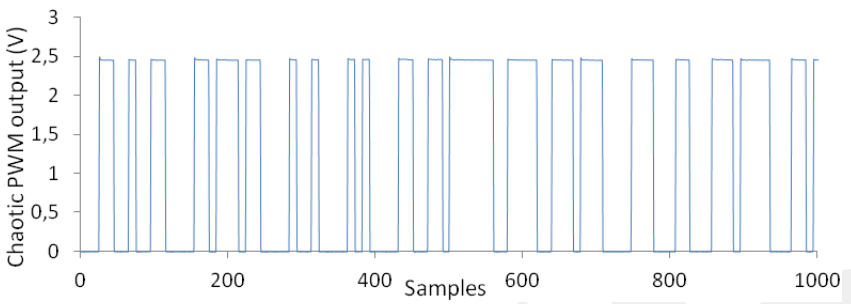

Fig. 17. Arduino results for the chaotic PWM implementation on the cross-coupled chaotic map $x(k+1) = -1.8y(k) + \text{sgn}(y(k))$, $y(k+1) = -1.8x(k) + \text{sgn}(x(k))$.

32 kilobytes of storage and 2 kilobytes of random access memory [Atmel, 2014]. The Arduino platform provides open-source hardware in design, architecture, collaboration, and philosophy. The Arduino Uno has six PWM outputs with a frequency at about 500 Hz. This speed can be increased up to several kHz for more sensitive applications. As a demonstration, the Arduino C source code for getting a chaos based PWM signal is provided below:

```
void setup() {
pinMode(3, OUTPUT); //pin3 is output
pinMode(7, OUTPUT); //pin7 is output
}
void loop() {
double r = 1.8, x = 0.1, val;
while (1) { //chaotic oscillator
x = -r * x + x/(abs(x)+0.01);
analogWrite(3, 160*(x+0.8)); // PWM output
delay(100); //100 ms delay
val = 0.0048 * analogRead(A0);
if (val >= (x + 1.3)) {
digitalWrite(7, HIGH);
}
else {
digitalWrite(7, LOW);
}}}
```

In the above program, the pin3 of the Arduino Uno is activated as a PWM output. The exponential function based chaotic map (3) is solved in the Arduino and its output is adjusted to give a duty cycle between 0% (corresponds to 0) and 100% (corresponds to 255). Then the resulting PWM output is read by the analog input pin (A0), and then the AND operation is applied between this signal and the chaotic sequence. Finally, the chaotic PWM output is sent to the pin7. The corresponding result is given in Fig. 16, which shows that the PWM sequence is chaotic (or random bit stream). The second chaotic PWM implementation result for the signum function based cross-coupled chaotic map (25) is shown in Fig. 17. Both chaotic PWM results show that the developed chaotic maps can easily be implemented in Arduino microcontroller environment for practical applications.

5. Conclusion

This work has presented novel chaotic maps based on some simple physical nonlinearities with Arduino microcontroller implementations. The chaotic maps are selected to be in the form of $x(k+1) = rx(k) + f(x(k))$ in which the nonlinear term of the model can be seen in nature, medicine and engineering systems. The variety, quality and dimension of

the chaotic maps are increased by weak coupling or cross-coupling of the same or different maps. The existences of the discrete-time chaotic systems are shown with positive Lyapunov exponents, bifurcation diagrams and web diagrams. The physical existence of the chaotic maps is demonstrated with Arduino realizations and chaotic pulse width modulation applications. It is shown that both one-dimensional and two-dimensional cross-coupled discrete chaotic systems can easily be implemented via off-the-shelf microcontrollers for engineering applications. Chaotic maps and microcontroller based realizations introduced in this work have high potential in many applications including cryptography, random number generations and chaotic mixing, and can also be used to model physical systems.

Acknowledgment

This work was supported by Research Fund of the Abdullah Gül University under project number FAB-2015-4.

References

Ablay, G. [2015a] "Chaos in PID controlled nonlinear systems," *J. Electr. Engin. Technol.* **10**, 1843–1850.

Ablay, G. [2015b] "Novel chaotic delay systems and electronic circuit solutions," *Nonlin. Dyn.* **81**, 1795–1804.

Acho, L. [2015] "A discrete-time chaotic oscillator based on the logistic map: A secure communication scheme and a simple experiment using Arduino," *J. Franklin Instit.* **352**, 3113–3121.

Atay, F. M., Jalan, S. & Jost, J. [2009] "Randomness, chaos, and structure," *Complexity* **15**, 29–35.

Atmel [2014] "Atmel 8-bit microcontrollers datasheet," *The Atmel AVR.*

Bahi, J. & Guyeux, C. [2013] *Discrete Dynamical Systems and Chaotic Machines*: *Theory and Applications* (CRC Press).

Balestra, M., Bellini, A., Callegari, S., Rovatti, R. & Setti, G. [2004] "Chaos-based generation of PWM-like signals for low-EMI induction motor drives: Analysis and experimental results," *IEICE Trans. Electron.* **E87-C**, 66–75.

Bilotta, E. & Pantano, P. [2009] "Discrete chaotic dynamics from Chua's oscillator: Chua machines," *Int. J. Bifurcation and Chaos* **19**, 1–115.

Chen, F.-J., Li, J.-B. & Chen, F.-Y. [2007] "Chaos for discrete-time RTD-based cellular neural networks," *Int. J. Bifurcation and Chaos* **17**, 4395–4401.

Chen, G. & Huang, Y. [2011] *Chaotic Maps*: *Dynamics, Fractals, and Rapid Fluctuations* (Morgan & Claypool Publishers).

Delgado-Restituto, M. & Rodriguez-Vazquez, A. [2002] "Integrated chaos generators," *Proc. IEEE* **90**, 747–767.

Fatehnia, M., Paran, S., Kish, S. & Tawfiq, K. [2016] "Automating double ring infiltrometer with an Arduino microcontroller," *Geoderma* **262**, 133–139.

Faugel, H. & Bobkov, V. [2013] "Open source hard- and software: Using Arduino boards to keep old hardware running," *Fus. Engin. Des.* **88**, 1276–1279.

Ferdoush, S. & Li, X. [2014] "Wireless sensor network system design using raspberry Pi and Arduino for environmental monitoring applications," *Procedia Comput. Sci.* **34**, 103–110.

Hamiche, H., Guermah, S., Saddaoui, R., Hannoun, K., Laghrouche, M. & Djennoune, S. [2015] "Analysis and implementation of a novel robust transmission scheme for private digital communications using Arduino Uno board," *Nonlin. Dyn.* **81**, 1921–1932.

Hussain, I. & Gondal, M. A. [2014] "An extended image encryption using chaotic coupled map and S-box transformation," *Nonlin. Dyn.* **76**, 1355–1363.

Ikeda, K. & Matsumoto, K. [1987] "High-dimensional chaotic behavior in systems with time-delayed feedback," *Physica D* **29**, 223–235.

Lakshmanan, M. & Senthilkumar, D. V. [2010] *Dynamics of Nonlinear Time-Delay Systems* (Springer, Berlin; Heidelberg; NY).

Lambi, D. [2015] "A new discrete chaotic map based on the composition of permutations," *Chaos Solit. Fract.* **78**, 245–248.

Liu, L. & Miao, S. [2015] "The complexity of binary sequences using logistic chaotic maps," *Complexity*, pp. 1–9.

Ortega-Zamorano, F., Jerez, J. M., Subirats, J. L., Molina, I. & Franco, L. [2014] "Smart sensor/actuator node reprogramming in changing environments using a neural network model," *Engin. Appl. Artif. Intell.* **30**, 179–188.

Pal, P., Debroy, S., Mandal, M. K. & Banerjee, R. [2014] "Design of coupling for synchronization in chaotic maps," *Nonlin. Dyn.* **79**, 2279–2286.

Radwan, A. G. [2013] "On some generalized discrete logistic maps," *J. Adv. Res.* **4**, 163–171.

Romero, N., Silva, J. & Vivas, R. [2014] "On a coupled logistic map with large strength," *J. Math. Anal. Appl.* **415**, 346–357.

Ruelle, D. [1997] "Chaos, predictability, and idealization in physics," *Complexity* **3**, 26–28.

Shi, Y. [2012] "Chaos in nonautonomous discrete dynamical systems approached by their induced systems," *Int. J. Bifurcation and Chaos* **22**, 1250284-1–12.

Shi, Y., Zhang, L., Yu, P. & Huang, Q. [2015] "Chaos in periodic discrete systems," *Int. J. Bifurcation and Chaos* **25**, 1550010-1–21.

Shrimali, M. D. & Banerjee, S. [2013] "Delayed q-deformed logistic map," *Commun. Nonlin. Sci. Numer. Simul.* **18**, 3126–3133.

Sprott, J. [2000] "Simple chaotic systems and circuits," *Amer. J. Phys.* **68**, 758–763.

Sprott, J. [2001] *Chaos and Time-Series Analysis*, 1st edition (Oxford University Press, Oxford, NY).

Strogatz, S. H. [2014] *Nonlinear Dynamics and Chaos*: *With Applications to Physics*, *Biology*, *Chemistry*, *and Engineering*, 2nd edition (Westview Press, Boulder, CO).

Tang, K.-S., Man, K., Zhong, G.-Q. & Chen, G. [2001] "Generating chaos via $x|x|$," *IEEE Trans. Circuits Syst.-I*: *Fund. Th. Appl.* **48**, 636–641.

Tian, C. & Chen, G. [2007] "Chaos in the sense of Li–Yorke in coupled map lattices," *Physica A* **376**, 246–252.

Tsonis, A. A. [1996] "Dynamical systems as models for physical processes," *Complexity* **1**, 23–33.

Wang, X.-Y. & Bao, X.-M. [2013] "A novel block cryptosystem based on the coupled chaotic map lattice," *Nonlin. Dyn.* **72**, 707–715.

Willeboordse, F. H. [2003] "The spatial logistic map as a simple prototype for spatiotemporal chaos," *Chaos* **13**, 533–540.

Wu, G.-C. & Baleanu, D. [2013] "Discrete fractional logistic map and its chaos," *Nonlin. Dyn.* **75**, 283–287.

Wu, G.-C., Baleanu, D. & Zeng, S.-D. [2014] "Discrete chaos in fractional sine and standard maps," *Phys. Lett. A* **378**, 484–487.

Zhang, Z., Ching, T., Liu, C. & Lee, C. [2012] "Comparison of chaotic PWM algorithms for electric vehicle motor drives," *IECON 2012 — 38th Ann. Conf. IEEE Industrial Electronics Society*, pp. 4087–4092.